Analytic description of the evolution of an axisymmetric flame surface

Analytic description of the evolution of an axisymmetric flame surface

M.L. Bondar[1] and J.H.M. ten Thije Boonkkamp

Eindhoven University of Technology, Department of Mathematics and Computer Science, PO Box 513, 5600 MB Eindhoven, The Netherlands

Abstract The dynamics of flame surfaces is of central interest in understanding combustion instabilities. Here, the G-equation formulation is used to assess the evolution of an axisymmetric flame surface subject to an unperturbed and to a perturbed gas flow, respectively. The flame is modelled using an extension of the models proposed in [1, 2]. The nonlinear G-equation for a constant modulus (S_L) of the laminar burning velocity is solved analytically using the method of characteristics. S_L is assumed constant only in a part of the domain and a mathematical rule is derived to stabilize the flame above the burner rim. By employing the solution of the G-equation the transient positions of a Bunsen flame reaching its stationary position are computed. After the flame stabilises, the flame response to an acoustic perturbation (the flame transfer function) is investigated.

Keywords Bunsen flame, G-equation, method of characteristics, flame stabilisation, transfer function

1 Introduction

In the past decade, the international requirements for the reduction of pollutant gas emissions, in particular nitrogen oxyde (NO_x), led to the development of combustion devices based on fuel lean premixed flames. The advantage of using lean premixed flames is that they have a relatively low temperature, resulting in low NO_x emissions. However, a fuel lean flame is prone to (self excited or externally excited) instabilities, e.g. as caused by the interaction with acoustic waves. Acoustic resonance in a system can lead to significant levels of noise, which is detrimental for the performance of the device and can even lead to structural damage [3, 4]. The design of noise-free combustion equipment is a challenging task whose achievement requires the understanding of the interaction between sound waves and flames.

One possible source of combustion noise originates in the coupling between perturbations in the heat release rate with the acoustic wave in the burner [5]. Thus, the acoustic waves perturb the flame, leading to oscillations in the heat release rate which in turn affect the acoustic waves. The heat release rate does not react instantaneously to the acoustic wave, but rather with a time lag. In the particular case where the phase difference between the oscillation in the heat release rate and the acoustic waves is less than 90 degrees, the acoustic waves gain energy (the so-called Rayleigh criterion), which can lead to the production of noise; see e.g. [6].

An appropriate model to study combustion instabilities is a Bunsen flame subject to an acoustic perturbation (acoustic velocity). The prediction of combustion noise requires a transfer function that correlates the perturbation of the heat release rate with the velocity perturbation. Due to the complexity of the equations describing a reactive flow, the complete numerical simulation of an oscillating flame is difficult and computationally demanding. Instead, the question of the transfer function can be addressed by making the following simplifying assumptions. The flame is considered to be a surface which separates the burnt gas from the unburnt one. In this paper this separating surface is referred to as the flame front. The flame front moves with the

[1]corresponding author `mbondar@win.tue.nl`

laminar burning velocity $\mathbf{S}_\mathrm{L}$, whose module S_L is constant, in the direction normal to its surface towards the unburnt gas. We further assume that the heat release rate is proportional to the area of the flame. The velocity field, which is assumed axial is modelled by a Poisseuile profile. In reality the acoustic velocity is not purely axial as assumed in our model. However the axial component of the velocity is dominant except near the base of the flame [7]. The gas flow is assumed to be unaffected by the flame and the effect of pressure perturbations on flame is neglected.

While the simplified model considered here does not entirely account for the complex behaviour of the flame, it allows us to investigate the response of the flame to flow perturbations. Using this model, the response of the flame to the flow perturbations can be determined by studying the changes in the area of the flame as function of time. Therefore, determining the instantaneous flame area and hence the location and shape of the flame front is of crucial importance in deriving the transfer function. The flame front can be mathematically described as a solution of a kinematic condition, the so-called G-equation. Ideally, in order to describe the dynamical behaviour of the flame, one needs the analytical solution of the G-equation for the general case of an arbitrary flow field. Due to the nonlinearity of the equation, this general solution cannot be obtained. As a consequence, several models were suggested that solve the G-equation at various levels of approximation. This includes, e.g., solving a linearized G-equation in the particular case where the laminar burning velocity has a constant direction that is normal to a stationary position of the flame [8, 2], or in the case where the flame is nearly parallel to the gas stream lines [1]. Other models use the method of characteristics to solve the G-equation for simple gas profiles [9, 10, 11].

In the present paper the transfer function of a flame subject to a perturbed Poisseuile flow is derived using a combined analytical and numerical approach. First, the stabilisation of a Bunsen flame above an axisymmetric burner is investigated. A real flame subject to an unperturbed laminar flow stabilises such that there is a balance between the flow velocity and the laminar burning velocity $\mathbf{S}_\mathrm{L}$ [12]. Away from the burner rim, S_L can be approximated with a constant. At the burner rim the flame looses heat resulting in a reduced S_L. Due to the constant S_L assumption, our model cannot account for the region close to the burner rim. Therefore, in order to stabilise the flame we will consider S_L constant only in the region where the gas velocity is larger than or equal to the laminar burning velocity and we derive a rule to stabilise the flame. The movement of the flame due to a Poisseuile flow from an initially zero flame front to its stationary position is determined by solving the G-equation analytically by using the method of characteristics. After stabilisation of the flame is achieved, the response of the flame to gas velocity perturbations of small amplitude is investigated. The perturbed flame front is approximated with an asymptotic expansion around its stationary position. Then, the equation which gives the flame front position is reduced to a system of simple advection equations which are solved numerically using the upwind scheme. Finally the transfer function is derived.

The paper is organized as follows. The derivation of the G-equation is given in Section 2, and in Section 3 we give a brief overview of the existing analytical solutions of the G-equation. The Charpit's equations for the G-equation are derived in Section 4 and they are solved in Section 5 for the particular case of a Poisseuile profile of the gas velocity. The response of the flame to the velocity perturbation and the derivation of the transfer function are presented in Section 6.

2 Derivation of the G-equation

Let us consider a scalar variable G, e.g. one of the species mass fractions or the temperature of the mixture. We define the flame front as the set of points $\mathbf{x}$ satisfying the relation $G(\mathbf{x}, t) = G_0$ for some relevant G_0. The flame front separates the burnt gas ($G(\mathbf{x}, t) > G_0$) from the unburnt gas ($G(\mathbf{x}, t) < G_0$). The flame front moves under the action of the flow velocity $\mathbf{v}$ and of the laminar burning velocity, $\mathbf{S}_\mathrm{L}$, which is normal to the flame surface and directed towards the unburnt gas

mixture. The velocity of the flame front $\mathbf{v}_\mathrm{f}$, can be written as

$$\mathbf{v}_\mathrm{f} = \mathbf{v} + \mathbf{S}_\mathrm{L} = \mathbf{v} + \mathrm{S}_\mathrm{L}\mathbf{n}, \qquad \mathbf{n} = -\nabla G/|\nabla G|, \tag{1}$$

where $\mathbf{n}$ is the unit normal on the flame surface, directed towards the unburnt gas mixture (Figure 1).

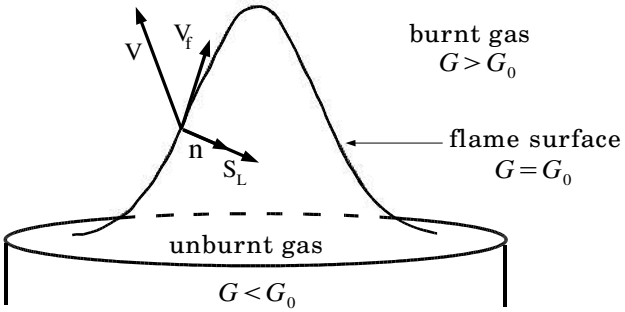

Figure 1: Flame front kinematics.

The motion of the flame front is described by the kinematic condition

$$\frac{\mathrm{d}G}{\mathrm{d}t} := \frac{\partial G}{\partial t} + (\mathbf{v}_\mathrm{f} \cdot \nabla)G = 0, \tag{2}$$

which means that a point on the flame front remains on the front for all time t. Substituting (1) in (2), the so-called G-equation is obtained

$$\frac{\partial G}{\partial t} + \mathbf{v} \cdot \nabla G = S_L|\nabla G|. \tag{3}$$

For an axisymmetric burner such as a Bunsen burner the assumption can be made, in the case of small amplitude perturbations, that the flame and the possible flame wrinkles are axisymmetric. Then, the surface of the flame can be described by the relation $G(r, z, t) = G_0$ where r and z are the radial and axial coordinates, respectively. Denoting the radial and the axial components of the gas velocity by $u(r, z, t)$ and by $v(r, z, t)$, respectively, the G-equation becomes

$$\frac{\partial G}{\partial t} + u\frac{\partial G}{\partial r} + v\frac{\partial G}{\partial z} = S_L\sqrt{\left(\frac{\partial G}{\partial r}\right)^2 + \left(\frac{\partial G}{\partial z}\right)^2}. \tag{4}$$

Since we are not interested to capture flame wrinkles, we can further assume that the flame is not locally vertical. This implies that $\partial G/\partial z > 0$ everywhere. Hence we can apply the implicit function theorem [13] to express z as a function of the other two variables, i.e. $z = \zeta(r, t)$. The partial derivatives of ζ with respect to r and t are then given by the expressions

$$\frac{\partial \zeta(r,t)}{\partial r} = -\frac{\partial G(r, \zeta(r,t), t)}{\partial r} \Bigg/ \frac{\partial G(r, \zeta(r,t), t)}{\partial z}, \tag{5a}$$

$$\frac{\partial \zeta(r,t)}{\partial t} = -\frac{\partial G(r, \zeta(r,t), t)}{\partial t} \Bigg/ \frac{\partial G(r, \zeta(r,t), t)}{\partial z}. \tag{5b}$$

Combining (4) and (5) we obtain the following equation for the location of the flame front $\zeta(r, t)$

$$\frac{\partial \zeta(r,t)}{\partial t} + u\frac{\partial \zeta(r,t)}{\partial r} - v + S_L\sqrt{\left(\frac{\partial \zeta(r,t)}{\partial r}\right)^2 + 1} = 0. \tag{6}$$

Once equation (6) has been solved, the area of the flame $A(t)$ can be computed from the formula

$$A(t) = 2\pi \int_0^R r\sqrt{\left(\frac{\partial \zeta}{\partial r}\right)^2 + 1}\mathrm{d}r. \tag{7}$$

3 Existing analytical models

Since the G-equation was introduced by Markstein in 1964 [14], several analytical and numerical approaches have been used to find a solution. Due to the nonlinearity of the equation, a general analytical solution for an arbitrary flow field is impossible to obtain. One possible solution to this problem is to consider an approximate, linear form of the G-equation that allows for an analytical solution for given flow fields. For simple gas profiles, e.g., with a quiescent flow or with a flat profile, another possible method is the method of characteristics. In what follows we review the solving of G equation by using the liniarization approach and by using the method of characteristics. The radial and the axial components of the gas velocity are denoted as u, v. The prime denotes a perturbation of the corresponding variable.

3.1 Solution obtained via linearization

The linearized G-equation may be obtained by assuming a constant laminar burning velocity, normal to a stationary position of the flame [8]. This assumption was used to study the dynamics and the shape of anchored V flames subject to a space-time perturbation of a flat profile of the gas velocity. The perturbation along the flame front was neglected, considering only the perturbation in the direction normal to the flame front. Working in a rectangular system of coordinates in which one of the axes is parallel to the steady flame position and using the Laplace transform, a linear PDE describing the perturbation of the flame front was derived and solved [8].

In the particular case of a Poiseuille flow, a solution of the linearized G-equation describing the front of a premixed laminar flame in a duct with radius R was obtained for flow perturbations harmonic in time and either uniform or non-uniform in space in [1]. The Poiseuille flow and its perturbations have the following expressions

$$u(r) = 0, \qquad v(r) = v_0\left(1 - \left(\frac{r}{R}\right)^2\right), \tag{8}$$

$$u'(r,t) = 0, \qquad v'(r,t) = \varepsilon \sin \omega t, \tag{9a}$$

or

$$u'(r,t) = 0, \qquad v'(r,t) = v_0\left(1 - \left(\frac{r}{R}\right)^2\right)\varepsilon \sin \omega t. \tag{9b}$$

where v_0 denotes the maximum velocity of the flow, and ε and ω are the amplitude and respectively the frequency of the perturbation. The square root term in (6) is approximated by $-\partial\zeta/\partial r$ assuming that the flame is nearly parallel to the stream lines therefore, $|\partial\zeta/\partial r| \gg 1$. The location of the flame front, $\zeta(r,t)$ is the contribution of the steady location of the flame $\overline{\zeta}(r)$ and of a perturbation $\zeta'(r,t)$. After enforcing flame stabilization at the wall by imposing $\zeta(R,t) = 0$, the steady location of the flame is obtained through a simple integration. Assuming as initial condition $\zeta(r,0) = \overline{\zeta}(r)$ the perturbation was obtained solving a linear PDE using the Laplace transform. As acknowledged in [15], the model has difficulties in describing the movement of the

flame at the burner rim and at the tip of the flame. Moreover, the model is limited to long flames with small cone angles and, unlike in experiment, the predicted stationary flame exhibits a tip that is not rounded.

Applying the same assumptions for the laminar burning velocity as in [8], the model by Fleifil et al. [1] was extended to flames with arbitrary cone angles [2]. In this case, the flame front position is given by the equation

$$\frac{\partial \zeta}{\partial t} - v + S_L \sin\alpha_0 - S_L \cos\alpha_0 \frac{\partial \zeta}{\partial r} = 0. \tag{10}$$

where α_0 denotes the half angle of the steady flame cone. The solution for an arbitrary time dependent flow field perturbation of a mean flat profile of the gas velocity was obtained for the perturbation $\zeta'(r,t)$ using the Laplace transform.

3.2 Solution obtained via the method of characteristics

The limitations of the linearized G-equation make it difficult to predict the right shape and movement of the flame front. Solving the nonlinear G-equation by the method of characteristics allows for the prediction of cusped flame fronts. Thus, the method of characteristics allowed, e.g., the investigation of cusped flame fronts subject to a velocity field given by

$$u(r,z,t) = \frac{r}{\sqrt{2}}\big(k\nu(z)\cos(\omega t - kz) - \frac{\mathrm{d}\nu(z)}{\mathrm{d}z}\sin(\omega t - kz)\big), \tag{11a}$$

$$v(r,z,t) = \big(1 + \sqrt{2}\nu(z)\sin(\omega t - kz)\big), \tag{11b}$$

where the dimensionless wave number k is equal to the frequency ω and $\nu(z)$ is the axial root-mean-squared (RMS) velocity [9]. By using the G-equation, the following kinematic equation in terms of $\tan(\theta)$, where θ is the angle between the tangent to the front at one of its points and the Oz axis could be derived

$$\frac{\partial}{\partial t}(\tan\theta) = \frac{\partial}{\partial z}\big[u + v\tan\theta - S_L(1+\tan\theta^2)^{1/2}\big]. \tag{12}$$

The solution of the equation (12) was further employed to assess how the the occurrence of cusps is affected by the magnitude of the mean flow velocity, by the flame speed, and by the amplitude of perturbations. In the case of long flames subject to harmonic disturbances of a flat profile of the gas velocity the solution of the G-equation via the method of characteristics was used to investigate the occurrence of cusped fronts as function of the length of the flame, perturbation amplitude, and of the flame Strouhal number [10].

4 Charpit's equations for the G-equation

Introducing the variables $p := \partial\zeta/\partial r$ and $q := \partial\zeta/\partial t$ we obtain the following expression for (6)

$$F(r,t,\zeta,p,q) := q + up - v + S_L\sqrt{p^2+1} = 0. \tag{13}$$

Equation (13) is a nonlinear, first order PDE that can be solved analytically by using the method of characteristics [16] for "simple" expressions for u, v and S_L. The solution is obtained by smoothly joining all the characteristic strips that emerge from the noncharacteristic initial strip defined by the initial condition $\zeta(r,0) = z_0(r)$, $p(r,0) = z_0'(r)$. This reduces (13) to a system of five ODEs, the so-called Charpit's equations. Let's introduce a parameter s along the characteristics and a parameter σ along the initial curve $t = 0$. In the following we use the notation $a(s;\sigma)$ for a

generic variable a to indicate that an expression only holds along a characteristic parametrized by s. The parameter σ denotes that the characteristic passes through the point $(0, \sigma)$. The notation $a(r, t)$ is used in the case where an expression holds in the $(r, t)-$ plane. Assuming a constant module S_L, for the laminar burning velocity the Charpit's equations and the initial conditions for a general flow field $u(r, z, t)$ and $v(r, z, t)$ become

$$\frac{\mathrm{d}r}{\mathrm{d}s} = u + S_L \frac{p}{\sqrt{p^2+1}}, \qquad r(0;\sigma) = \sigma, \tag{14a}$$

$$\frac{\mathrm{d}t}{\mathrm{d}s} = 1, \qquad t(0;\sigma) = 0, \tag{14b}$$

$$\frac{\mathrm{d}\zeta}{\mathrm{d}s} = p\left(u + S_L \frac{p}{\sqrt{p^2+1}}\right) + q, \qquad \zeta(0;\sigma) = z_0(\sigma), \tag{14c}$$

$$\frac{\mathrm{d}p}{\mathrm{d}s} = -\left[p\frac{\partial u}{\partial r} - \frac{\partial v}{\partial r} + p\left(p\frac{\partial u}{\partial z} - \frac{\partial v}{\partial z}\right)\right], \qquad p(0;\sigma) = z_0'(\sigma), \tag{14d}$$

$$\frac{\mathrm{d}q}{\mathrm{d}s} = -\left[p\frac{\partial u}{\partial t} - \frac{\partial v}{\partial t} + q\left(p\frac{\partial u}{\partial z} - \frac{\partial v}{\partial z}\right)\right], \qquad q(0;\sigma) = q_0(\sigma). \tag{14e}$$

Note that $q(s;\sigma)$ can be eliminated from (14c) using (13) and that the initial condition $q_0(\sigma)$ follows from the other initial conditions. From (14b) we simply obtain $t(s;\sigma) = s$, and it remains for us to solve (14a), (14c) and (14d). Since $p = -\tan\beta$, where β is the angle between the horizontal line and the tangent to $\zeta(r, t)$, the system reduces to

$$\frac{\mathrm{d}r}{\mathrm{d}t} = u + S_L \frac{p}{\sqrt{p^2+1}} = u - S_L \sin\beta, \qquad r(0;\sigma) = \sigma, \tag{15a}$$

$$\frac{\mathrm{d}\zeta}{\mathrm{d}t} = v - S_L \frac{1}{\sqrt{p^2+1}} = v - S_L \cos\beta, \qquad \zeta(0;\sigma) = z_0(\sigma), \tag{15b}$$

$$\frac{\mathrm{d}p}{\mathrm{d}t} = -p\frac{\partial u}{\partial r} + \frac{\partial v}{\partial r} - p\left(p\frac{\partial u}{\partial z} - \frac{\partial v}{\partial z}\right), \qquad p(0;\sigma) = z_0'(\sigma). \tag{15c}$$

The Charpit's equations (15) for a Poiseuille flow will be solved in the next section.

5 Solution for a Poiseuille flow

The flow in a cylindrical duct may be approximated with a Poiseuille flow described by (8). Here, we extend the models proposed in [1, 2] by taking into consideration flames that have arbitrary cone angles and by using a laminar burning velocity of constant modulus that does not have a constant direction to a stationary position of the flame front. The variables in (15) are scaled as follows

$$r^* := r/R, \quad t^* := t/\tilde{t}, \quad \sigma^* := \sigma/R, \quad \zeta^* := \zeta/R, \tag{16}$$

where $\tilde{t} := R/S_L$. The dimensionless system (we omitted the $*$) is

$$\frac{\mathrm{d}r}{\mathrm{d}t} = \frac{p}{\sqrt{p^2+1}}, \qquad r(0;\sigma) = \sigma, \tag{17a}$$

$$\frac{\mathrm{d}\zeta}{\mathrm{d}t} = \hat{v}(1-r^2) - \frac{1}{\sqrt{p^2+1}}, \qquad \zeta(0;\sigma) = z_0(\sigma), \tag{17b}$$

$$\frac{\mathrm{d}p}{\mathrm{d}t} = -2\hat{v}r, \qquad p(0;\sigma) = z_0'(\sigma), \tag{17c}$$

where $\hat{v} := v_0/S_L$ being typically in the interval $\hat{v} \in (1, 10]$. The formal solution procedure for the system (17) is as follows. First, we find the expression for $p(r;\sigma)$. Second, we determine the location of the characteristics in an implicit form $t = t(r;\sigma)$, and we find the location of the flame front $\zeta(r;\sigma)$ along the characteristics. Third, we invert the implicit relation $t = t(r;\sigma)$, to find $\sigma = \sigma(r,t)$ and replace σ in the expression for $\zeta(r;\sigma)$ to find the position $\zeta(r,t)$ of the flame front.

From (17a) and (17c) the following differential equation is obtained

$$\frac{p}{\sqrt{p^2+1}}\mathrm{d}p = -2\hat{v}r\mathrm{d}r. \tag{18}$$

Since $p \leq 0$, we obtain by integrating (18)

$$p(r;\sigma) = -\sqrt{\left(c(\sigma) - \hat{v}r^2\right)^2 - 1}, \tag{19}$$

where $c(\sigma) := \sqrt{1 + z_0'(\sigma)^2} + \hat{v}\sigma^2 \geq 1$. Substituting expression (19) for p in (17a) and applying the corresponding initial condition we obtain the integral form of the location of the characteristics, i.e.,

$$t(r;\sigma) = -\int_\sigma^r \frac{c(\sigma) - \hat{v}x^2}{\sqrt{\left(c(\sigma) - \hat{v}x^2\right)^2 - 1}}\,\mathrm{d}x. \tag{20}$$

The integral on the right hand side term of (20) cannot be evaluated analytically. However, it is possible to reformulate (20) in terms of elliptic integrals of first and second kind [17, 18], which are implemented in most of the existing technical computing software. These are defined by respectively

$$F(\phi, m) := \int_0^\phi \frac{\mathrm{d}x}{\sqrt{1 - m^2\sin^2 x}}\,\mathrm{d}x, \quad E(\phi, m) := \int_0^\phi \sqrt{1 - m^2\sin^2 x}\,\mathrm{d}x. \tag{21}$$

where the number m is the *modulus* and the variable integration limit ϕ is the *argument* of the elliptic integrals. To simplify the expressions for $t(r;\sigma)$ and $\zeta(r;\sigma)$ that follow, we introduce the auxiliary variables

$$k(\sigma) := \sqrt{\frac{c(\sigma) - 1}{c(\sigma) + 1}}, \quad \psi(r;\sigma) := \arcsin\left(r\sqrt{\frac{\hat{v}}{c(\sigma) - 1}}\right), \quad \tau(\sigma) := \psi(\sigma;\sigma), \tag{22a}$$

$$\mathcal{E}(\psi, \tau, k) := E(\psi, k) - E(\tau, k), \quad \mathcal{F}(\psi, \tau, k) := F(\psi, k) - F(\tau, k). \tag{22b}$$

With these variables the relation (20) becomes

$$t(r;\sigma) = \frac{1}{\sqrt{\hat{v}(c(\sigma) + 1)}}\mathcal{F}(\psi, \tau, k) - \sqrt{\frac{c(\sigma) + 1}{\hat{v}}}\mathcal{E}(\psi, \tau, k). \tag{23}$$

Combining (17a) and (17b) we obtain

$$\frac{\mathrm{d}\zeta}{\mathrm{d}r} = \frac{\hat{v}(1 - r^2)\sqrt{p^2 + 1} - 1}{p}. \tag{24}$$

Integrating (24) and using (20) we obtain the following integral expression for the location of the flame front along the characteristics

$$\zeta(r;\sigma) = z_0(\sigma) + \hat{v}t(r;\sigma) + \int_\sigma^r \frac{1 + \hat{v}x^2(c(\sigma) - \hat{v}x^2)}{\sqrt{\left(c(\sigma) - \hat{v}x^2\right)^2 - 1}}\,\mathrm{d}x. \tag{25}$$

Expressing the integral in (25) in terms of elliptic integrals and using the notation in (22), we obtain the following expresion for $\zeta(r;\sigma)$,

$$\zeta(r;\sigma) = z_0(\sigma) + \hat{v}t(r;\sigma) + \left(\frac{c(\sigma)\sqrt{c(\sigma)+1}}{3\sqrt{\hat{v}}}\right)\mathcal{E}(\psi,\tau,k) + \left(\frac{2-c(\sigma)}{3\sqrt{\hat{v}(c(\sigma)+1)}}\right)\mathcal{F}(\psi,\tau,k) \\ -\frac{1}{3}\left(r\sqrt{(c(\sigma)-\hat{v}r^2)^2-1} - \sigma\sqrt{(c(\sigma)-\hat{v}\sigma^2)^2-1}\right). \tag{26}$$

To find the location of the flame front $\zeta(r,t)$, σ as a function of r and t is needed. Therefore relation (20), or equivalently (23), has to be inverted. This is possible only if

$$J(r;\sigma) := \frac{\partial t(r;\sigma)}{\partial \sigma} \neq 0. \tag{27}$$

Because of the complicated formula in (23), it is difficult to investigate the sign of $J(r;\sigma)$ for a general initial profile of the flame front. However, we are interested to study the movement of the flame front for the special case $z_0(r) = 0$. Then the variable $k(\sigma)$, $\psi(r;\sigma)$ and $\tau(\sigma)$ reduce to

$$k(\sigma) = \sqrt{\frac{\hat{v}\sigma^2}{\hat{v}\sigma^2+2}}, \quad \psi(r;\sigma) = \arcsin\left(\frac{r}{\sigma}\right), \quad \tau(\sigma) = \frac{\pi}{2}. \tag{28}$$

In this case (27) becomes

$$J(r;\sigma) = \frac{1}{\sigma\sqrt{\hat{v}(\hat{v}\sigma^2+2)}}\left(\mathcal{F}(\psi,\tau,k) - (\hat{v}\sigma^2+1)\mathcal{E}(\psi,\tau,k) + \right. \\ \left. \frac{r\hat{v}(\sigma^2-r^2)(\hat{v}\sigma^2+1) + r(\hat{v}\sigma^2+2)}{\sqrt{(\sigma^2-r^2)(\hat{v}\sigma^2+2)(\hat{v}(\sigma^2-r^2)+2)}}\right). \tag{29}$$

For $0 < r < \sigma$ we have $J(r;\sigma) > 0$, which makes it possible to use the implicit function theorem and therefore to express σ as a function of r and t. This also proves that no cusps form in the flame front.

The flame moves under the influence of the Poisseuile flow and of the laminar burning velocity whose modulus is constant. At the edge of the tube a region exists where the laminar burning velocity is larger than the gas velocity and the flame is pushed into the tube. This entry of the flame into the tube does not agree with the known movement of a real flame. To overcome the unrealistic behaviour of the modelled flame we assume that the S_L is constant only in the region where the gas velocity is larger than the laminar burning velocity, i.e. $0 \leq r \leq \delta$, where δ is such that $\hat{v}(1-\delta^2) = 1$. This gives

$$\delta = \sqrt{1-\hat{v}^{-1}}. \tag{30}$$

Because it is not possible to invert (23) analytically we use the following numerical approach. We introduce a uniform grid for the space and time domains, i.e. $r_j = j\Delta r$, $j = 1,\ldots,M$, $t^n = n\Delta t$, $n = 0,\ldots,N$, with the grid size $\Delta r = \delta/(M-1)$ and time step $\Delta t = 1/N$. For given r_j and t^n we compute the corresponding σ_j^n from (20) using the secant method. From the geometrical viewpoint this means that at a certain moment in time t^n we trace back along the characteristic which passes through r_j, and we find the intersection point σ_j^n of the characteristic with the initial line $t = 0$ (Figure 2). The location $\zeta(r_j,t^n)$ is given by $\zeta(r_j,t^n) = \zeta(r_j;\sigma_j^n)$. For all n, when $\sigma_j^n > \delta$ the location of the flame front satisfies $\zeta(r_j,t^n) < \zeta(r_j,t^{n-1})$. This observation together with the initial condition implies that when $\sigma_j^n > \delta$ the flame is either in the tube or the flame will enter the tube at a following time level.

To stabilise the flame above the tube we impose the following rule. If for some r_k the corresponding $\sigma_k^n > \delta$ we compute the location of the flame front according to $\zeta(r_k,t^n) = \zeta(r_k;\delta)$.

This rule implies that the flame is fixed above the burner. Indeed, $\zeta(\delta, t^n) = \zeta(r_M; \sigma_M^n)$ and since $\delta = r_M < \sigma_M^n$, from the previous condition together with the initial condition $z_0(\sigma) = 0$ we conclude that $\zeta(\delta, t^n) = \zeta(\delta; \delta) = 0$ for $n = 0, \ldots, N$. Therefore, the previous rule implies the boundary condition $\zeta(\delta, t) = 0$ for $t \geq 0$. From the geometrical viewpoint these rule means to cut off the characteristics with the straight line passing through the points $(\delta, 0)$, (δ, t^n), (Figure 2) and to take into consideration only the characteristics which are inside the domain $[0, \delta] \times [0, t^n]$.

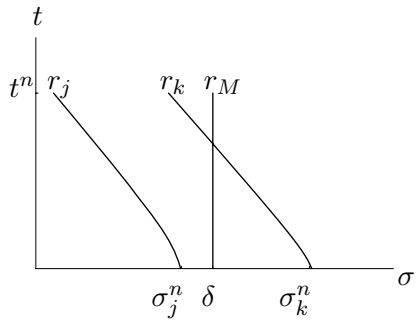

Figure 2: The characteristics through (r_j, t^n) and (r_k, t^n)

According to the present analytical model the flame reaches a stationary position after starting from an initial flat profile at the time level $t^N = 1$. The stationary position of the flame is within discretization error equal to the steady solution of (6) subject to the boundary condition $\zeta_0(\delta) = 0$, which has the following expression

$$\zeta_0(r) = \int_r^\delta \sqrt{\hat{v}^2(1 - x^2)^2 - 1}\, \mathrm{d}x, \tag{31}$$

with δ given in (30), or in terms of elliptic integrals

$$\zeta_0(r) = \frac{\delta}{3\lambda}\left(2\hat{v}\mathcal{E}(\alpha, \beta, \lambda) - 2\mathcal{F}(\alpha, \beta, \lambda) - (\hat{v} - 1)\sin\beta\cos\beta\sqrt{1 - \lambda^2\sin^2\beta}\right). \tag{32}$$

Here the variables α, β and λ are given by

$$\alpha = \frac{\pi}{2}, \quad \beta(r) = \arcsin\left(\frac{r}{\delta}\right), \quad \lambda = \frac{\delta}{\sqrt{1 + \hat{v}^{-1}}}. \tag{33}$$

An illustration of a transient flame position given by the system (17) is given in Figure 3.

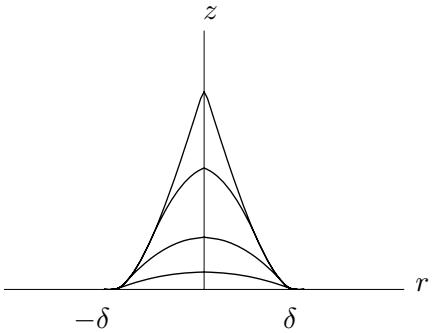

Figure 3: Transient Bunsen flame reaching its stationary position. The intermediary positions depicted here are for values $\tilde{t} \in \{0.0333,\ 0.1,\ 0.233,\ 1\}$ and $\hat{v} = 5$.

6 Perturbed Poiseuille profile

After the flame stabilises above the burner, we apply a perturbation of the gas velocity that is harmonic in time and and nonuniform in space i.e.,

$$u'(r,t) = 0, \qquad v'(r,t) = v_0\left(1 - \left(\frac{r}{R}\right)^2\right)\varepsilon \sin \omega t, \tag{34}$$

where ω is the angular frequency and $0 < \varepsilon \ll 1$. Substituting the perturbed velocity field into (6) the equation for the location of of the flame front becomes

$$\frac{\partial \zeta}{\partial t} - v_0\left(1 - \left(\frac{r}{R}\right)^2\right)(1 + \varepsilon \sin \omega t) + S_L\sqrt{\left(\frac{\partial \zeta}{\partial r}\right)^2 + 1} = 0. \tag{35}$$

By choosing to work with dimensional variables we can control the length of the interval on which the flame stabilises such that it corresponds to the radius of a real burner. Equation (35) cannot be solved analytically for $\varepsilon \neq 0$. Instead, to derive a system of linear advection equations which can be easily solved numerically, we apply the following asymptotic expansion for ζ,

$$\zeta(r,t) = \zeta_0(r,t) + \varepsilon\zeta_1(r,t) + \varepsilon^2\zeta_2(r,t) + \cdots \tag{36}$$

Substituting expression (36) into equation (35) and collecting terms of the same order leads to a system of equations. The small amplitude of the perturbation allows us to take into consideration only the leading, first and second order equations of the system. The leading order equation of the system in dimensional form is

$$\frac{\partial \zeta_0}{\partial t} - v_0\left(1 - \left(\frac{r}{R}\right)^2\right) + S_L\sqrt{\left(\frac{\partial \zeta_0}{\partial r}\right)^2 + 1} = 0. \tag{37}$$

Due to the assumption that perturbation in the gas velocity is introduced after the stabilisation of the flame above the burner rim, the leading order term in (36) can be replaced by the steady solution of (37) satisfying $\zeta_0(R\delta) = 0$, given by

$$\zeta_0(r) = \int_r^{R\delta} \sqrt{\hat{v}^2\left(1 - \left(\frac{x}{R}\right)^2\right)^2 - 1}\ \mathrm{d}x. \tag{38}$$

The first and the second order equations of the system are

$$\frac{\partial \zeta_1}{\partial t} - S_L\frac{\sqrt{v(r)^2 - {S_L}^2}}{v(r)}\frac{\partial \zeta_1}{\partial r} = \frac{v'(r,t)}{\varepsilon}, \tag{39a}$$

$$\frac{\partial \zeta_2}{\partial t} - S_L\frac{\sqrt{v(r)^2 - {S_L}^2}}{v(r)}\frac{\partial \zeta_2}{\partial r} = \frac{-{S_L}^4\left(\frac{\partial \zeta_1}{\partial r}\right)^2}{2v(r)^3}. \tag{39b}$$

with $v(r)$ defined in (8) and $v'(r,t)$ defined in (34). Although (39a) and (39b) are linear first order advection equations, analytic solutions of these two equations are difficult to obtain. Therefore a numerical solution is derived. After imposing the following initial (IC) and boundary conditions (BC),

$$\text{IC} \quad \zeta_1(r,0) = 0, \quad \zeta_2(r,0) = 0, \tag{40a}$$

$$\text{BC} \quad \zeta_1(R\delta,t) = 0, \quad \zeta_2(R\delta,t) = 0, \tag{40b}$$

we solve (39a) and (39b) using the upwind scheme and the explicit Euler approach for the source term. Since it is necessary to compute the variation of the area in time, the time interval needs to be large enough to capture the oscillatory behaviour of the area perturbation. For a time interval $t = 0$ to 8 s, $S_L = 0.35$ ms^{-1} and a tube radius of 0.01 m we choose $\Delta r = 10^{-4}$ and $\Delta t = (8/3)10^{-4}$ to give a CFL number equal to 0.933. By combining the solutions of the leading, first and second order equation we obtain an analytical-numerical description of the perturbed flame front. The resulting perturbation of the flame front around the stationary position is depicted in Figure 4.

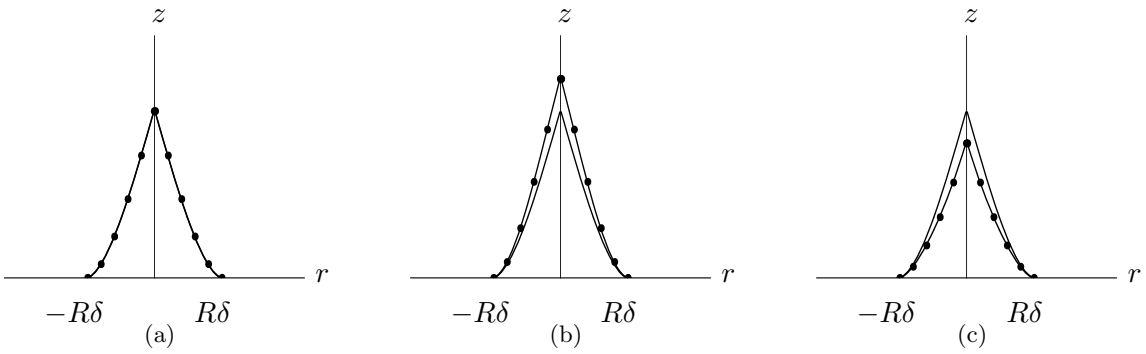

Figure 4: Oscillation of the flame front (solid line with bullets) around the stationary position (solid line). The following parameters were used: v_0=3 ms^{-1}, $S_L = 0.35$ ms^{-1}, $\omega = 50$Hz, $\varepsilon = 0.05$ and $\delta = 0.01$ m (a) $t = 0$s, (b) $t = 0.05$s, (c) $t = 0.15$s.

The area of the perturbed flame can be computed from (7) using the trapezoid rule. An illustration of the variation of the area in time is presented in Figure 5.

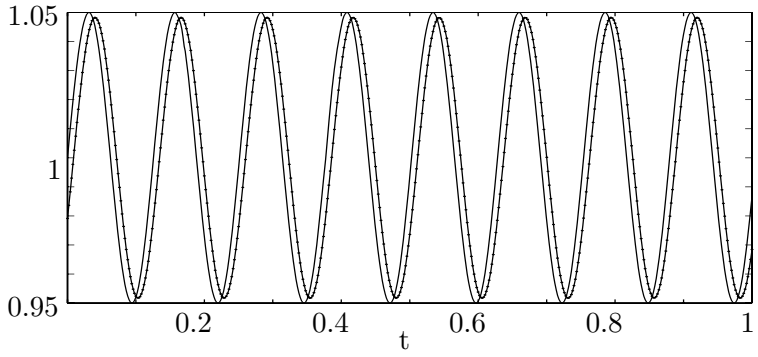

Figure 5: Variation in time of the area of the flame (solid line with bullets) and of the velocity of the flow in the center of the duct (solid line). The flame area and the velocity were normalized with the initial values. The following parameters were used: v_0=3 ms^{-1}, $S_L = 0.35$ ms^{-1}, $\omega = 50$Hz, $\varepsilon = 0.05$ and $\delta = 0.01$ m.

Figure 5 indicates that the time variation of the area of the flame can be fitted to a sine function by the means of the least-squares approximation. The transfer function of the flame $H(\omega)$ is computed over the range of angular frequencies $\omega = 10$Hz to 300Hz. The magnitude of the transfer function $|H(\omega)|$ is given by

$$|H(\omega)| = (Q_a/Q_0)/(v_a/v_0), \tag{41}$$

where Q_a and v_a are the amplitude of the heat release rate oscillations and respectively the velocity fluctuations, having as initial values Q_0 and respectively v_0. Under the assumption that

the heat release rate is proportional with the area of the flame, $|H(\omega)|$ reduces to

$$|H(\omega)| = (A_a/A_0)/(v_a/v_0), \tag{42}$$

where A_a and A_0 are the amplitude and respectively the initial value of the perturbed flame area. The angle of the transfer function $\angle H(\omega)$ is the phase difference between the area perturbation and the velocity perturbation in the centre of the duct. Because the phase difference becomes approximately -90 degrees and the magnitude decays to 0 when the frequency increases, it is natural to compare the flame transfer function with the transfer function of a first-order system having the form

$$\tilde{H}(i\omega) = \frac{\alpha}{\alpha + i\omega}, \tag{43}$$

where α is a fitting parameter. The best approximation of our data is for $\alpha = 90$. In the small frequency range the phase of the flame transfer function closely follows the one of the first order system, whereas the magnitude is larger. The phase of the flame transfer function tends to -90 degrees faster than a first order model. The discrepancy between the flame model and the approximative transfer function can be diminished by considering a higher order system in equation (43).

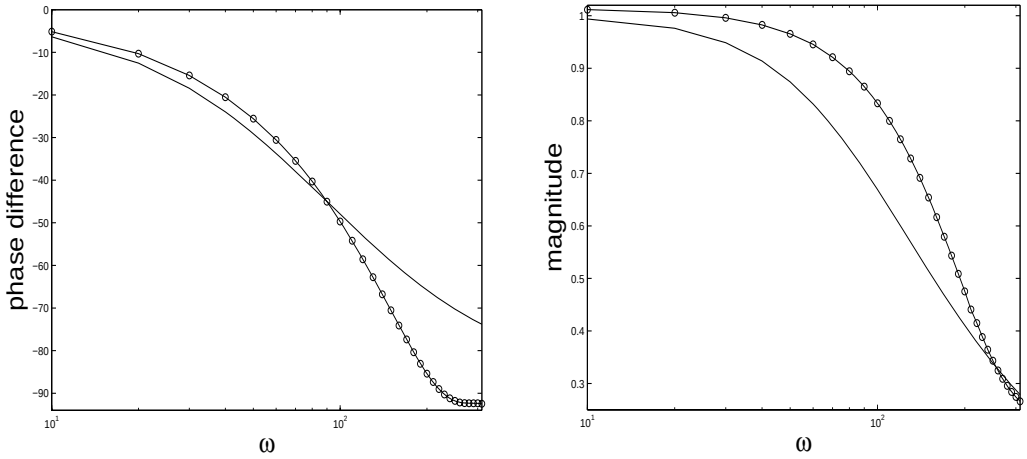

Figure 6: The phase difference and the magnitude of the transfer function. The solid curves were obtained with the first-order approximation, and the empty circles denote the flame model. The following parameters were used: v_0=3 ms^{-1}, ε=0.05, $S_L = 0.35$ ms^{-1}, δ=0.01 m

The flame transfer function computed here is similar with the ones derived with the analytical models from [2, 1]. As pointed out in [2] the model correctly predicts the flame behaviour for small frequencies, but fails for frequencies in the intermediate and high frequency range. The current model could be improved by considering the dependence of the laminar burning velocity on the geometry of the flame and/or include the heat exchange with the burner at the foot of the flame.

7 Conclusions

The kinematic condition describing the motion of a flame front (the G-equation) subject to a Poisseuile flow was solved analytically by using the method of characteristics. Analytical expressions in terms of elliptic integrals were given for the location of characteristics and for the location of the flame front along the characteristics. In order to use a constant S_L we restricted

the flame to the region in which the gas velocity is larger than the laminar burning velocity. To stabilise the flame a mathematical rule was derived in computing the position of the flame front along the characteristics. This rule enabled us to compute the transient flame front position of a Bunsen flame while reaching its stationary position. The results are validated by the fact that the stationary position is the same as the steady solution of the G-equation. The solution of the equation giving the flame front position of a perturbed flame was approximated with an asymptotic expansion from which we retained the leading, the first and the second order terms. The area of the flame as computed using the trapezoid rule exhibits an oscillatory behaviour that could be fitted to a sine function using a least-squares approximation. The frequency dependence of the phase difference and of the magnitude of the transfer function was computed and compared to the results obtained with the first-order approximation. The flame transfer function computed here agrees with the transfer functions computed with the analytical models from [2, 1]. Concurrent with previous observations [2], the flame model described here correctly predicts the behaviour of the flame for the small frequency range. However, in the high-frequency range the flame model gives a phase difference of the transfer function that converges to -90 in disagreement with the experiments. The current model could be improved by considering the dependence of the laminar burning velocity on the flame curvature and strain and/or include the heat exchange with the burner at the foot of the flame. To achieve this improvement the numerical integration of the G-equation is required.

Acknowledgments

The authors would like to thank Dr. P. Kagan for useful discussion and Dr. K. Schreel for critically reading the manuscript. This research is supported by the Technology Foundation STW, applied science division of NWO and the technology programme of the Ministry of Economic Affairs.

References

[1] M. Fleifil, A. M. Annaswamy, Z. A. Ghoneim, and A. F. Gnoniem. Response of a laminar premixed flame to flow oscillations: A kinematic model and thermoacustic instability results. *Combustion and Flame*, 106:487–510, 1996.

[2] S. Ducruix, D. Durox, and S. Candel. Theoretical and experimental determination of the transfer function of a laminar premixed flame. *Proceedings of the Combustion Institute*, 28:765–773, 2000.

[3] S. Candel. Combustion dynamics and control:Progress and challenges. *Proceedings of the Combustion Institute*, 29:1–28, 2002.

[4] T. Lieuwen and K. McManus. That elusive hum. *Mechanical Engineering*, 124:53–55, 2002.

[5] Lord Rayleigh. *The theory of sound*, volume 2, chapter XVI, pages 226–227. Dover Publications, USA, 2nd edition, 1945.

[6] A. Putnam and W. Dennis. Burner oscillation of the gause-tone type. *Journal of the Acoustical Society of America*, 29:716–725, 1954.

[7] T. Lieuwen. Acoustic near-field characteristics of a conical, premixed flame. *Journal of the Acoustical Society of America*, 113:167–177, 2003.

[8] L. Boyer and J. Quinard. On the dynamics of anchored flames. *Combustion and Flame*, 82:51–65, 1990.

[9] F. Baillot, A. Bourehla, and D. Durox. The characteristics method and cusped flame fronts. *Combustion Science and Technology*, 112:327–350, 1995.

[10] T. Lieuwen. Nonlinear kinematic response of premixed flames to harmonic velocity disturbances. *Proceedings of the Combustion Institute*, 30:In press, 2004.

[11] C. J. Sung, C. J. Sun, and C. K. Law. Analytic description of the evolution of two-dimensional flame surfaces. *Combustion and Flame*, 107:114–124, 1996.

[12] B. Lewis and G. von Elbe. *Combustion, Flames and Explosions of Gases*, pages 220–224. Academic Press Inc., New York and London, 2nd edition, 1961.

[13] S.G. Krantz and H.R. Parks. *The implicit function theorem*. Birkhäuser, Boston.Basel.Berlin, 2002.

[14] G. H. Markstein. *Nonsteady flame propagation*. Pergamon Press, Oxford, 1964.

[15] C. Dieteren. *Response of axisymmetric laminar premixed flames to an acoustic field*. Technische Universiteit Eindhoven, Eindhoven, 1997. Master Thesis.

[16] J. Kevorkian. *Partial Differential Equations. Analytical Solution Techniques*, chapter 6, pages 322–385. Chapman and Hall, New York-London, 1990.

[17] M. Abramowitz and I.A. Stegun. *Handbook of mathematical functions, with formulas, graphs, and mathematical tables*, chapter 17, pages 587–626. Dover Publications, USA, 1974.

[18] P. F. Byrd and M. D. Friedman. Handbook of elliptic integrals for engineers and scientists. Springer-Verlag, Berlin. Göttingen. Heidelberg, 1971.